

Variational wave functions for vortex states in a Bose Superfluid

Jian-Ming Tang

Department of Physics, University of Washington
Box 351560, Seattle WA 98195-1560
(submitted to PRB on February 25, 1999)

Following the quantization scheme developed by Peierls, Yoccoz, and Thouless, an improved variational many-body wave function of the vortex state can be obtained by using the superposition of degenerate states. The overlap matrix elements between two Feynman wave functions localized at different points are calculated, and an integral equation is developed for the weighting function. In two dimensions a close analogy between a moving vortex and a moving electron in a magnetic field is made. A numerical study is conducted for the Bose superfluid using the Hartree ground-state wave function. We show the improved Feynman wave functions for the ground states of the vortex and also for the excited states corresponding to the cyclotron motion. The fluid density is finite at the vortex axis and the vorticity is distributed in the core region. The effective vortex mass defined by the inverse of the Landau level spacing is shown to be logarithmically divergent with the system size.

PACS numbers: 67.40.Vs, 67.40.-w, 02.30.Rz

I. INTRODUCTION

Quantized vortices have been recognized to play essential roles in various phenomena of superfluids, such as the critical velocity of the superflow,^{1,2} quantization of circulation,²⁻⁴ mutual friction in the phenomenological two-fluid model,^{5,6} and Berezinskii-Kosterlitz-Thouless phase transition.^{7,8} The naive picture of a vortex state drawn from classical hydrodynamics is a filament with non-vanishing vorticity immersed in an irrotational fluid.⁹ This semi-classical model has been quite successful for describing static vortices or vortex rings except that a phenomenological parameter corresponding to the radius of the core region has to be introduced.¹⁰ In liquid ⁴He the core size is estimated to be comparable to the inter-atomic spacing,^{2,11} and any classical theory fails to account for its origin. In the case of a moving vortex filament, the existence of long-ranged phase correlation in a superfluid changes the response function of the fluid,¹² and in the mean time affects its motion.¹³ In most cases, the correlation simply renormalizes the total density into the superfluid density. Therefore, a quantum theory is required for understanding the origin of the microscopic core as well as for studying the dynamics of the vortex filament. Phenomenological theory using a charged particle in a central gauge field has been very intriguing for understanding the motion of a vortex in two dimensions, but the effective parameters, such as the mass and the viscosity, are still not well understood.¹⁴⁻¹⁸

A variational approach is one of the important methods to study such a quantum many-body problem. The trial wave function in its simplest form based on the above model is proposed by Feynman.² It has a singularity at the center of the vortex core, which is usually removed by introducing a density profile that vanishes at the vortex center, with the healing length determined

variationally.¹⁹ This constraint imposed on the fluid density is present in most theories because the vorticity is strictly confined to a line so that the circulation is quantized along any closed path around it. This semi-classical quantization condition can not be applied on the atomic scale, and therefore needs to be relaxed in the vicinity of the vortex core. Besides using the variational principle, an inhomogeneous condensed state is proposed as a solution for the weakly interacting bosons by Gross and Pitaevskii,^{20,21} who show that the condensate vanishes linearly toward the center. In this case, it is argued by Fetter that the excitations of particle pairs are important within the core region since the condensate fails to be the dominate component.²² As a result, he conjectures that the fluid density is roughly constant throughout the system.

Numerical *ab initio* calculations using the variational approach have been pushed forward recently,²³⁻²⁷ but mainly focus on the structure of a static vortex, i.e. a vortex in its ground state. It is probably less known that the variational wave functions are also very useful for studying the collective behaviors, such as translation, rotation and oscillation, of a many-body system. This method for constructing the variational wave functions of collective motions is initially proposed by Hill and Wheeler,²⁸ and also by Redlich and Wigner.²⁹ It is then implemented by Peierls, Yoccoz and Thouless in order to incorporate the collective modes of nuclei in a shell-model description.^{30,31} In this paper we follow Peierls and Yoccoz to develop a new set of trial wave functions for the vortex states of a bosonic system, which can be used to investigate the excited vortex states. These trial wave functions also provide a different view to the core structure and overcome the difficulty of the semi-classical quantization. The fluid density at the vortex axis is shown to be finite, and the vorticity is distributed

within the core region. Similar observations on the non-vanishing density have also been reported in some other variational calculations by partially shifting the coordinates or introducing a set of “shadow” variables.^{24,25,27}

In classical hydrodynamics a moving vortex in two dimensions is very similar to a classical moving electron in a magnetic field. There is a transverse Magnus force acting on the vortex in analogy with the Lorentz force. Its motion creates a dipolar velocity field known as the backflow, and consequently leads to an effective mass associated with the displaced fluid. It then moves in a circular orbit with an arbitrary radius but a fixed angular frequency.⁹ In the quantum theory an electron moves in an effective harmonic potential and has eigenstates with different angular momenta if the central gauge is chosen. These energy eigenstates shift up and down from the simple harmonic spectrum according to their individual angular momentum, and form highly degenerate Landau levels. On the other hand, there is no corresponding theory for such vortex states in the superfluids. Experimental evidence for the existence of such excitations has been shown in a more complicated situation, where the cyclotron motion is coupled to the standing wave along the vortex filament.³² It is the purpose of the present paper to show that there are highly degenerate Landau levels consisting of vortex states in a superfluid. The energy spectrum and the “wave functions” however are different than what we expect from such an intuitive analogy.

In section II a brief description of the basic idea for our method will be given, and an integral equation for the trial wave function is presented. Then we consider the simplest trial function with a uniform ground state in section III. In section IV we show the structure of a static vortex. Since we use a simplified ground state, our results only show the qualitative features for the density and velocity distributions. The excited states and the effective mass are discussed in section V.

II. GENERATOR COORDINATES

The wave function for an uniform superfluid flow can be obtained by performing a Galilean transformation on the ground state

$$\exp \left(i \frac{m}{\hbar} \sum_{j=1}^N \int d\mathbf{r}_j \cdot \mathbf{v}_s \right) \Psi_{\text{gs}}(\mathbf{r}_1, \dots, \mathbf{r}_N), \quad (1)$$

where m is the atomic mass, \mathbf{v}_s is the flow velocity, \mathbf{r}_j is the position vector of each particle and N is the total number of particles. This wave function can be generalized as an approximation for a superflow with a velocity field slowly varying in space

$$\mathbf{v}_s(\mathbf{r}) = \frac{\hbar}{m} \nabla \phi(\mathbf{r}), \quad (2)$$

where $\phi(\mathbf{r})$ is the velocity potential. One can try to apply this approximation to the state with a single vortex line fixed at a point \mathbf{r}_0 , and the velocity potential is simply the azimuthal angle $\theta(\mathbf{r} - \mathbf{r}_0)$ with respect to the vortex center. This is the so called Feynman wave function²

$$\Psi_{\mathbf{r}_0}(\mathbf{r}_1, \dots, \mathbf{r}_N) = \exp \left[i \sum_{j=1}^N \phi(\mathbf{r}_j, \mathbf{r}_0) \right] \Psi_{\text{gs}}. \quad (3)$$

In an infinite homogeneous superfluid these semi-classical wave functions centered at different points are degenerate because of the translational symmetry. It is known that one can improve on the variational energy further by using the superposition of these degenerate ones as the new trial wave function. Like the shell-model wave functions for nuclei, these basis functions, namely equation (3), are already a quite good approximation for vortices. Consequently, the collective coordinates, such as the position of the vortex, are treated more like quantum variables other than classical parameters. However, in the case of translational motion of nuclei, this scheme is still too simple to yield the correct dependence between the energy and the linear momentum. It is suggested by Peierls and Thouless that the trial wave function has to be a linear combination of shell-model wave functions with both varying positions and velocities.³¹ In the case of a vortex in a superfluid both corrections have been suggested in the numerical studies through quite different reasonings. Introducing the “shadow” variables is similar to varying the position of a vortex,^{25,27} and adding the backflow corresponds to varying the velocity.^{24,26} Nevertheless, they have only been considered for the lowest energy state.

In order to study the excited collective modes, we propose a trial wave function for the vortex following Peierls and Yoccoz, which is a superposition of the Feynman wave functions centered at different positions. We do not consider trial functions with different velocities at the present stage because including them introduces more parameters, and complicates the problem. For example, the velocity potential for a vortex with a hard core of radius a in an infinite system is modified as follows,

$$\phi(\mathbf{r}) = \theta - \frac{ma^2 v}{\hbar r} \cos(\theta - \theta_v). \quad (4)$$

where v and θ_v represent the magnitude and direction of the moving velocity of the vortex, and a is the hard core radius. It is the additional backflow term in equation (4) that gives rise to the classical hydrodynamical effective mass. We will see later that the long-ranged correlation dominates for a quantized vortex, and the backflow only contributes as a minor correction.

We start with a generic Hamiltonian with a two-body potential plus a confining potential from the boundary

$$H = -\frac{\hbar^2}{2m} \sum_{i=1}^N \nabla_i^2 + \frac{1}{2} \sum_{i,j=1}^N V(\mathbf{r}_i - \mathbf{r}_j) + V_b. \quad (5)$$

For simplicity, we consider a single vortex centered at $\mathbf{r}_0 = (x_0, y_0)$ in a finite two-dimensional disk with radius R . The corresponding classical problem in hydrodynamics can be solved easily by using an image vortex with the opposite circulation located at a distance R^2/r_0 from the origin, where the velocity potential is

$$\phi(\mathbf{r}_j, \mathbf{r}_0) = \tan^{-1} \frac{y_j - y_0}{x_j - x_0} - \tan^{-1} \frac{y_j - R^2 y_0 / r_0^2}{x_j - R^2 x_0 / r_0^2}. \quad (6)$$

Since the position vector consists of continuous variables, we use a weighting function $f_{n,l}(\mathbf{r}_0)$ as the coefficient for the superposition. The angular dependence of the weighting function follows directly from the cylindrical symmetry of the system

$$\Psi_{n,l}(\mathbf{r}_1, \dots, \mathbf{r}_N) = \int d^2 \mathbf{r}_0 f_{n,l}(r_0) e^{i l \theta_0} \Psi_{\mathbf{r}_0}, \quad (7)$$

where n is the principal quantum number and l is the angular momentum. Follow the convention by Feynman,³³ we define

$$F_{n,l}(\mathbf{r}_1, \dots, \mathbf{r}_N) = \int d^2 \mathbf{r}_0 f_{n,l}(r_0) e^{i \Phi_l(\mathbf{r}_1, \dots, \mathbf{r}_N, \mathbf{r}_0)}, \quad (8)$$

where the complete phase factor is

$$\Phi_l(\mathbf{r}_1, \dots, \mathbf{r}_N, \mathbf{r}_0) = l \theta_0 + \sum_{j=1}^N \phi(\mathbf{r}_j, \mathbf{r}_0). \quad (9)$$

The expectation value of the Hamiltonian relative to the ground state energy E_{gs} is

$$\begin{aligned} \varepsilon_n &= \langle \Psi_{n,l} | H | \Psi_{n,l} \rangle - E_{\text{gs}} \\ &= \frac{\frac{\hbar^2}{2m} \int d^2 \mathbf{r}_1 \dots d^2 \mathbf{r}_N \sum_{j=1}^N |\nabla_j F_{n,l}|^2 \Psi_{\text{gs}}^2}{\int d^2 \mathbf{r}_1 \dots d^2 \mathbf{r}_N |F_{n,l}|^2 \Psi_{\text{gs}}^2}. \end{aligned} \quad (10)$$

The inter-atomic potential does not appear explicitly in the above formula, therefore all information about the interaction is hidden inside the ground-state wave function. By varying the weighting function $f_{n,l}(r'_0)$ to minimize ε_n , we can obtain an integral equation for $f_{n,l}(r_0)$,

$$\int dr_0 K_l(r'_0, r_0) f_{n,l}(r_0) = 0, \quad (11)$$

where the kernel of this integral equation is

$$\begin{aligned} K_l(r'_0, r_0) &= 2\pi r_0 \int d\Delta\theta_0 \int d^2 \mathbf{r}_1 \dots d^2 \mathbf{r}_N \\ &\quad e^{i(\Phi_l - \Phi'_l)} \left[\sum_{j=1}^N \nabla_j \phi' \nabla_j \phi - \frac{2m\varepsilon_n}{\hbar^2} \right] \Psi_{\text{gs}}^2. \end{aligned} \quad (12)$$

The integrand only depends on the relative angle, $\Delta\theta_0 = \theta'_0 - \theta_0$, and each term in the summation is the same as

others by Bose symmetry. The overlap integral between two semi-classical wave functions has been calculated previously by Niu *et al.*,¹⁵ but I do not agree that equation (12) can be approximated by a simple Gaussian with a fixed width.

III. HARTREE APPROXIMATION

The simplest model for the ground-state wave function is the Hartree approximation for an infinite homogeneous superfluid. It is a constant function, and is a good approximation for a dilute system with repulsive interaction. In applying it to our finite system, the boundary effect is completely neglected. The multiple N -particle integral in the kernel equation (12) is thus reduced to a simple product of one-particle integrals

$$\begin{aligned} K_l(r'_0, r_0) &= 2\pi r_0 \int d\Delta\theta_0 e^{-il\Delta\theta_0} \left[\frac{1}{A} \int d^2 \mathbf{r} e^{i(\phi - \phi')} \right]^{N-1} \\ &\quad \left[\frac{N}{A} \int d^2 \mathbf{r} \nabla \phi' \nabla \phi e^{i(\phi - \phi')} - \frac{2m\varepsilon_n}{\hbar^2 A} \int d^2 \mathbf{r} e^{i(\phi - \phi')} \right], \end{aligned} \quad (13)$$

where A is the area of the disk. The only length scale that comes in explicitly in this model is the inter-atomic distance, namely $\sigma = R/\sqrt{N}$, and this is going to be used as the basic length unit in our later discussion. Numerical calculations suggest that σ is about 2.7 Å at the saturation density of a two-dimensional helium film.³⁴ The energy scale associated with this length scale is $\hbar^2/m\sigma^2 \approx 1.7K$. Other length scales must come in through the ground-state wave function because there is no extra cut-off introduced in our scheme. The explicit cut-off becomes necessary if we want to include trial wave functions of moving vortices.

Equation (13) contains two different integrals; one is the overlap between two semi-classical bases, and the other one is the same overlap weighted by the kinetic energy. The phase factor of the overlap integrand can be rewritten as the opening angle between two vortex centers

$$\phi - \phi' = \Theta + \Theta_I, \quad (14)$$

where Θ is the angle spanned from $\mathbf{r} - \mathbf{r}'_0$ to $\mathbf{r} - \mathbf{r}_0$, and Θ_I is the corresponding angle with respect to the images. The integrand is first expanded with respect to r_0/R and r'_0/R up to the second order $O(d^2/R^2)$, where $d = |\mathbf{r}_0 - \mathbf{r}'_0|$ is the separation between the two vortex centers. It is a self-consistent condition that we only look for localized weighting functions later. The integral is evaluated by dividing the integration range into three distinct regions. The inner most one $A_1 = \pi d^2/4$ is the circle centered at $\mathbf{r}_c = (\mathbf{r}_0 + \mathbf{r}'_0)/2$ with diameter d

$$\begin{aligned} &\int_{A_1} d^2 \mathbf{r} \left[e^{i(\Theta + \Theta_I - \Delta\theta_0)} - 1 \right] \\ &= -(1.66386 + \pi) \left(\frac{d}{2} \right)^2 + O(R^{-2}), \end{aligned} \quad (15)$$

where an extra phase factor $\exp(-i\Delta\theta_0)$ is included for the convenience of notation. The numerical constant in equation (15) is calculated by first carrying out the angular part of the integral analytically using elliptic integrals (see Appendix A for details.) The second one $A_2 = \pi(R - r_c)^2 - A_1$ is the ring centered at \mathbf{r}_c from the inner radius $d/2$ to the outer radius $R - r_c$

$$\begin{aligned} \int_{A_2} d^2\mathbf{r} \left[e^{i(\Theta + \Theta_I - \Delta\theta_0)} - 1 \right] \\ = - \left(2 \ln \frac{2R}{d} + \frac{5}{2} \right) \pi \left(\frac{d}{2} \right)^2 + O(R^{-1}), \end{aligned} \quad (16)$$

where the factor $5/2$ is due to the presence of the image vortices. The last one A_3 is simply the rest of the area $A - A_1 - A_2$ like a thin crescent moon

$$\int_{A_3} d^2\mathbf{r} \left[e^{i(\Theta + \Theta_I - \Delta\theta_0)} - 1 \right] = -i\pi r_0 r'_0 \sin \Delta\theta_0 + O(R^{-1}). \quad (17)$$

Putting equations (15)-(17) together, we obtain

$$\begin{aligned} \frac{1}{A} \int_A d^2\mathbf{r} e^{i(\Theta + \Theta_I - \Delta\theta_0)} \\ = 1 - \left(\frac{1}{2} \ln \frac{2R}{d} + \alpha \right) \left(\frac{d}{R} \right)^2 - \frac{i r_0 r'_0 \sin \Delta\theta_0}{R^2}, \end{aligned} \quad (18)$$

where $\alpha = 7/8 + 1.66386/4\pi = 1.00741$. In the infinite system limit the image vortices contributes the constant in equation (16) and the overall phase factor $\exp(i\Delta\theta_0)$, which cancels the phase factor that we put in the above equations on purpose. The appearance of this phase factor is closely related to the fact that l is the total angular momentum of the system, which will become clear after we work out the final form of the kernel.

The other integral, which contains the kinetic energy factor, can also be written in the form with open angles

$$\nabla\phi' \nabla\phi \simeq \frac{\cos\Theta}{|\mathbf{r} - \mathbf{r}_0| |\mathbf{r} - \mathbf{r}'_0|}. \quad (19)$$

The image vortices do not have much effect in this case besides the overall phase. It can potentially lift the degeneracy of energy levels, but the contribution relative to the leading term is at most of the order $O(R^{-2})$. The first approximation to this integral is $2\pi \ln(2R/d)$ from the region A_2 . The correction at the same order must be a dimensionless number since there is no other dimensional parameters other than d

$$\int_A d^2\mathbf{r} \nabla\phi' \nabla\phi e^{i\Theta} = 2\pi \ln \frac{2R}{d} + \pi\beta, \quad (20)$$

where $\pi\beta = -1.92801$. This number can be found by evaluating the integral for any particular choice of d . The contribution from the region A_3 is negligible. Therefore, we reach the final form of the kernel in the large N limit,

$$\begin{aligned} K_l(r'_0, r_0) = 2\pi r_0 \int d\Delta\theta_0 \left[2 \ln \frac{2R}{d} + \beta - \frac{2m\varepsilon_n}{\hbar^2} \right] \\ \times S_l(r'_0, r_0, \Delta\theta_0), \end{aligned} \quad (21)$$

where

$$\begin{aligned} S_l(r'_0, r_0, \Delta\theta_0) = \exp \left\{ - \left(\frac{1}{2} \ln \frac{2R}{d} + \alpha \right) d^2 \right. \\ \left. - i [r_0 r'_0 \sin \Delta\theta_0 - (N - l) \Delta\theta_0] \right\}. \end{aligned} \quad (22)$$

IV. STRUCTURE OF VORTEX STATES

The final integration over $\Delta\theta_0$ in the kernel equation (21) cannot be carried out in a systematic way through a series expansion because the integrand is not an analytic function. Assuming that the system size is sufficiently large, equation (22) can be approximated by a simple Gaussian form

$$\exp \left[- \left(\frac{1}{2} \ln \frac{2R}{d} + \alpha \right) d^2 \right] \simeq \exp(-Cd^2), \quad (23)$$

where

$$C = \ln \sqrt{2R} + \alpha + \frac{1}{4} \ln \left(\ln \sqrt{2R} + \alpha \right), \quad (24)$$

and the following constraints are required

$$R \gg r_0, r'_0 \gg \ln R \gg \sigma \gg d. \quad (25)$$

In this case equation (22) is a sharply peaked function where the peak is along the line of $r_0 = r'_0$ and $\Delta\theta_0 = 0$. It is reasonable to seek for the weighting function of the ground state of the vortex that also possess a Gaussian form

$$f_{0,l}(r_0) = \mathcal{N}(l) \exp \left[-\lambda^2 (r_0 - r_v)^2 \right], \quad (26)$$

as long as the peak of it is well away from the origin $r_v \gg \lambda^{-1}$, in which r_v and λ are the parameters to be determined, and $\mathcal{N}(l)$ is the normalization constant.

The integration variables in equation (11) are first changed to $x = r_0 - r'_0$ and $y = r'_0 \Delta\theta_0$, and then the integration range is extended to infinity so that the integral is approximately like a two-dimensional Gaussian integral

$$\begin{aligned} \iint dx dy [\ln(x^2 + y^2) + \delta] \exp \left[-\lambda^2 (x + r'_0 - r_v)^2 \right. \\ \left. - C(x^2 + y^2) - iy \left(x + r'_0 - \frac{N-l}{r'_0} \right) \right] = 0, \end{aligned} \quad (27)$$

where

$$\delta = \frac{2m\varepsilon_0}{\hbar^2} - 2\ln(2R) - \beta . \quad (28)$$

An orthogonal transformation is performed to change the Gaussian integral into the following canonical form

$$\int_{-\infty}^{\infty} d\mu \int_{-\infty}^{\infty} d\nu [\ln(\mu^2 + \nu^2) + \delta] \times \exp[-\xi(\mu - \mu_0)^2 - \eta(\nu - \nu_0)^2 + \tau] = 0 . \quad (29)$$

Since the logarithm is a slowly varying function, the integral equation leads to

$$\ln(\mu_0^2 + \nu_0^2) + \delta = 0 , \quad (30)$$

where

$$\begin{aligned} \mu_0^2 + \nu_0^2 &= \frac{8\lambda^2(2C + \lambda^2)(r'_0 - r_v)(r'_0{}^2 - N + l)}{r'_0 [4C(C + \lambda^2) + 1]^2} \\ &+ \frac{[1 - 4(C + \lambda^2)^2](r'_0{}^2 - N + l)^2}{r'_0{}^2 [4C(C + \lambda^2) + 1]^2} \\ &+ \frac{4\lambda^4(4C - 1)(r'_0 - r_v)^2}{[4C(C + \lambda^2) + 1]^2} , \end{aligned} \quad (31)$$

with the help of saddle-point approximation. We then expand the argument of the logarithm with respect to r'_0 around r_v because equation (26) is significant only around that point. Setting the coefficients of the first and second order terms to zero, we obtain a pair of linear equations for the input parameters. The solution is $r_v = \sqrt{N - l}$ and $\lambda = 1$, which is self-consistent with the assumption that the weighting function is localized away from the origin.

The zeroth order of the expansion also vanishes after substituting in the above solution, which makes it obsolete to use equation (30) for calculating the energy directly. With a more careful treatment by substituting the solution back to the integral equation (29), the energy of the ground state of the vortex is obtained

$$\begin{aligned} \varepsilon_0(R) &= \frac{\hbar^2}{2m} \int d^2\mathbf{r}_1 \cdots d^2\mathbf{r}_N \sum_j \nabla_j \Psi_{0,l}^* \nabla_j \Psi_{0,l} \\ &= \frac{\hbar^2}{2m} (2\ln 2R + \beta + \gamma_E + \ln C) . \end{aligned} \quad (32)$$

Equation (32) explicitly shows that the energy is independent of azimuthal quantum number l . These degenerate ground states of the vortex with different angular momenta form the first Landau level. It is obvious from the functional form of r_v on l that the degeneracy of the first Landau level is the total number of particles, $l = 1 \dots N$. It is interesting to keep in mind that the system has its maximum angular momentum $N\hbar$, when the vortex is located at the center of the disk. The normalization constant for the state with angular momentum l is calculated in the limit of large system size

$$\mathcal{N}(l)^2 \simeq \frac{\ln \sqrt{2R} + \alpha}{\pi^2 \sqrt{2\pi(N - l)}} . \quad (33)$$

Instead of trying to find other different forms of weighting functions with more fitting parameters, we choose to solve the integral equation (11) numerically, which is rewritten in the following matrix form

$$[\mathbf{K}_I(l, R) - \varepsilon_n(R)\mathbf{K}_{II}(l, R)]\mathbf{f}(n, l) = 0 . \quad (34)$$

Each matrix element of $\mathbf{K}_I(l, R)$ and $\mathbf{K}_{II}(l, R)$ can be calculated from equation (21) as a one-variable integral. By diagonalizing $\mathbf{K}_{II}^{-1}(l, R)\mathbf{K}_I(l, R)$, we can solve the eigenvectors $\mathbf{f}(n, l)$ and the corresponding eigenvalues $\varepsilon_n(R)$ simultaneously. The calculation is carried out for several different chosen sizes of matrices, and an extrapolation to the continuum limit is performed to obtain the final result.

It is sufficient to only work out the \mathbf{K} matrices partially because the magnitudes of elements far away from the diagonal are significantly smaller. This is the reason why we can carry out the calculation for a fairly large system size $R = 10^6\sigma$ without increasing the sizes of the matrices much, and maintain the same numerical accuracy. The typical square matrix that we use has a few hundred elements on one side. Selected numerical results for the weighting functions are shown in figures 1–3, and the energy spectrum is shown in figure 4. The weighting functions are very similar to the single-particle wave function in one-dimensional quantum mechanics, in which the number of nodal points increases as the energy goes up. We show explicitly in equation (34) that the excitation energy is independent of the angular momentum and the weighting function does not depend on system size. The existence of higher Landau levels is only proved numerically because we do not have any analytic result other than equation (32), which is only valid for the ground states of the vortex with $l \ll N$.

Despite the crude approximation that we use for the ground-state wave function, namely a constant, our results show qualitatively similar features in comparing with the Monte Carlo calculation in liquid helium. The density profile is calculated using the following formula

$$\begin{aligned} \rho_{n,l}(r) &= \int \frac{d\theta}{2\pi} \int d^2\mathbf{r}_1 \cdots d^2\mathbf{r}_N \Psi_{n,l}^* \sum_j \delta(\mathbf{r} - \mathbf{r}_j) \Psi_{n,l} \\ &= \frac{N}{A} \int d\Delta\theta_0 \int dr_0 r_0 f_{n,l}(r_0) \int dr'_0 r'_0 f_{n,l}(r'_0) \\ &\quad S_l(r'_0, r_0, \Delta\theta_0) \int d\theta e^{i(\phi - \phi')} , \end{aligned} \quad (35)$$

and several results for $n = 0$ states are shown in figure 5.

The particle density at the vortex axis is finite in general. Equation (35) even seems to suggest that it is uniform in the infinite system limit. For the finite system, the density at the core is less than the asymptotic value. This is in good agreement with the conjecture by Fetter.²² The fraction density at the core center shown by

Monte Carlo calculations are generally smaller than our estimation.^{24,25,27} Our result certainly fails to reproduce the detail features, such as the small oscillations in space around the average density, because the size of particles is neglected in the Hartree ground state.

The current density is given by

$$\begin{aligned} j_{n,l}(r) &= -\frac{i\hbar}{2m} \int \frac{d\theta}{2\pi} \hat{\theta} \cdot \int d^2\mathbf{r}_1 \cdots d^2\mathbf{r}_N \\ &\quad \Psi_{n,l}^* \sum_j \left[\delta(\mathbf{r} - \mathbf{r}_j) \vec{\nabla} - \vec{\nabla} \delta(\mathbf{r} - \mathbf{r}_j) \right] \Psi_{n,l} \\ &= \frac{\hbar N}{mA} \int d\Delta\theta_0 \int dr_0 r_0 f_{n,l}(r_0) \int dr'_0 r'_0 f_{n,l}(r'_0) \\ &\quad \int \frac{d\theta}{2r} \Im_m \left[e^{-i\phi'} \left(\frac{\partial}{\partial\theta} e^{i\phi} \right) S_l(r'_0, r_0, \Delta\theta_0) \right]. \quad (36) \end{aligned}$$

A few distributions for the first Landau level are shown in figure 6. The current density drops down to zero at the center, and shortly backs to the asymptotic behavior $1/r$.

V. LANDAU LEVELS AND EFFECTIVE MASS

In the framework of classical hydrodynamics, a moving vortex in two dimensions has a characteristic cyclotron frequency

$$\omega = \frac{\rho\kappa}{M_{\text{eff}}}, \quad (37)$$

where ρ is the fluid density, κ is the circulation, and M_{eff} is the effective mass of the vortex. An analogy with an electron in a magnetic field suggests that the energy levels for a vortex are highly degenerate, and the level spacing is simply a constant $\hbar\omega$. The degeneracy has been justified by our numerical calculation, but the prediction for level spacings is nevertheless incorrect as we have already seen in figure 4 that they tend to increase among higher excited states. As a matter of fact, the theories in their quantized forms of these two systems are quite different. First of all, the Hamiltonian of the electron is gauge-dependent, and is not necessarily spherically symmetric. If we choose the central gauge, the electron is moving in an effective harmonic potential created by the uniform magnetic field, and the angular momentum of it can be either positive or negative. However, the harmonic potential created by the image vortex is negligible for a sufficiently large system, and the angular quantum number of a vortex state only takes positive values ranging from one to the total number of particles in the fluid. Secondly, the excitation energy is strictly proportional to the number of nodes in the radial weighting function for a vortex state, while for an electron state it obtains an additional shift according to its angular momentum.

Even though the analogy does not provide an exact one-to-one mapping between two systems, the energy levels shown in figure 4 still correspond to the cyclotron motion of the vortex. We can try to define the dynamical

effective mass, which is one of the important parameters in the point-particle description of the vortex, as the inverse of the energy-level spacing

$$M_{\text{eff}} = \frac{\hbar\rho\kappa}{\Delta E}, \quad (38)$$

where ΔE is the level spacing. This is a very rough definition, and needs further refinement because the level spacings are not simply constant. It is nevertheless good enough to see the finite size scaling by looking at how energy levels scale with the system size. We plot the inverse energy-level spacings with respect to the system size in figure 7, which clearly shows that the corresponding effective mass diverges logarithmically.

This property is specific for a quantized vortex because a classical one has a finite effective mass. Through the calculation suggests that it is due to the long-ranged phase correlation in the superfluid. Although our calculation is done rigorously only for the dilute interacting bosons, we would like to argue that the scaling behavior is going to persist even in the strongly interacting system for the following reason. This scaling behavior is closely connected with the logarithmic factor inside the overlapping integral, which implies that all the trial wave functions are orthogonal in the infinite system limit. It is not surprising that the kernel equation (21) is significant non-zero only when the separation of two vortex center coordinates are close to each other. However, it behaves quite differently from the kernel function of a short-ranged correlated system such as the nucleus because the peak width scales logarithmically with the system size. This dependence is different from the logarithmic dependence on the system size of the kinetic energy, where the later is known from the classical theory. This non-trivial dependence is essential for understanding that a quantized vortex has a divergent mass. The orthogonality is due to the phase factor associated with the vortex. Any two shifted vortex wave functions eventually lose their phase coherence at the large distance, even though they are only displaced by a small amount. Interaction might change the detail dependence on the vortex coordinates or the constant, but could only changes the short distance physics. For sufficient large system size, the logarithm is going to be the dominate term, so is the scaling behavior. In real system the logarithm will be cut off at a certain length scale, where the condensate loses its phase coherence.

In conclusion, we present a set of variational wave functions for the vortex states. A detail calculation is carried out for the dilute interacting boson system. The core radius is shown to be about the same magnitude as the particle spacing in contrast to the Gross-Pitaevskii solution of the non-linear Schrödinger equation, which has a “macroscopic” core. The density is finite at the vortex axis and the vorticity is distributed in the core region. In the form of weighting functions, we also present the excited states of the vortex corresponding to the cyclotron

motion. Furthermore, vortex states with different angular momenta are degenerate and form Landau levels. The inverse of the spacing between Landau levels, which may be used to define the dynamical effective mass, diverges logarithmically with the system size.

ACKNOWLEDGMENTS

It is a pleasure to thank David Thouless for initiating the idea of this work and stimulating discussions. The author is also grateful to Ping Ao for valuable comments and suggestions. This work was partially supported by NSF Grant No. DMR-9528345.

APPENDIX A: ANGULAR INTEGRALS

The overlapping integral in equation (13) disregarding the image vortices can be written in the following form using complex variables

$$\int d^2 \mathbf{r} e^{i\Theta} = \int dr \int d\theta \sqrt{\frac{(re^{i\theta} - r_0 e^{i\theta_0})(re^{-i\theta} - r'_0 e^{-i\theta'_0})}{(re^{i\theta} - r'_0 e^{i\theta'_0})(re^{-i\theta} - r_0 e^{-i\theta_0})}} \quad (A1)$$

$$= \int dr \sqrt{\frac{C}{B}} \oint \frac{dz}{iz} \sqrt{\frac{(z - A)(z - B)}{(z - C)(z - D)}}, \quad (A2)$$

where

$$A = \frac{r_0}{r} e^{i\theta_0} \quad B = \frac{r}{r'_0} e^{i\theta'_0} \quad C = \frac{r}{r_0} e^{i\theta_0} \quad D = \frac{r'_0}{r} e^{i\theta'_0}. \quad (A3)$$

The integration contour is along the unit circle and crosses through the two Riemann sheets. There are always two branch points inside the circular contour and two outside it. Using the formula for elliptic Integrals in Appendix B, we can calculate the angular part of the integral by suitably deforming the contours

$$\begin{cases} 2\pi \sqrt{\frac{r_0}{r'_0}} e^{-i\Delta\theta_0/2} + 4C_1 [\Pi(n_1, k) - \Pi(n_2, k)] & \text{for } r > r_0, r'_0 \\ 2\pi \sqrt{\frac{r_0}{r'_0}} e^{-i\Delta\theta_0/2} - 4C_1 \left\{ [\Pi(n_1, k) - \Pi(n_2, k)] + \frac{1}{\sqrt{k}} \left[\Pi\left(\frac{1}{n_3}, \frac{1}{k}\right) - \Pi\left(\frac{1}{n_4}, \frac{1}{k}\right) \right] \right\} & \text{for } r_0 < r < r'_0 \\ 2\pi \sqrt{\frac{r_0}{r'_0}} e^{-i\Delta\theta_0/2} - 4C_1 [\Pi(n_3, k) - \Pi(n_4, k)] & \text{for } r < r_0, r'_0 \end{cases}, \quad (A4)$$

where

$$C_1 = \frac{r^2 - r_0 r'_0 e^{-i\Delta\theta_0}}{\sqrt{(r^2 - r_0^2)(r^2 - r'_0^2)}}, \quad (A5)$$

$$n_1 = \frac{r'_0 (r_0 e^{-i\Delta\theta_0} - r'_0)}{r^2 - r'_0^2}, \quad (A6)$$

$$n_2 = \frac{r^2 (r_0 - r'_0 e^{i\Delta\theta_0})}{r_0 (r^2 - r'_0^2)}, \quad (A7)$$

$$k = \frac{-r^2 (r_0^2 + r'_0^2 - 2r_0 r'_0 \cos \Delta\theta_0)}{(r^2 - r_0^2)(r^2 - r'_0^2)}, \quad (A8)$$

and n_3, n_4 are simply n_1, n_2 with r_0, r'_0 interchanging their roles. See figure (8) for one particular choice of the integration contour.

The kinetic energy term can be done in the similar way,

$$\begin{aligned} & \int d^2 \mathbf{r} \nabla \phi' \nabla \phi e^{i\Theta} \\ &= \int dr \int d\theta \frac{(re^{i\theta} - r_0 e^{i\theta_0})(re^{-i\theta} - r'_0 e^{-i\theta'_0}) + (re^{i\theta} - r'_0 e^{i\theta'_0})(re^{-i\theta} - r_0 e^{-i\theta_0})}{2(re^{i\theta} - r'_0 e^{i\theta'_0})(re^{-i\theta} - r_0 e^{-i\theta_0}) |re^{i\theta} - r_0 e^{i\theta_0}| |re^{-i\theta} - r'_0 e^{-i\theta'_0}|} \end{aligned} \quad (\text{A9})$$

$$= \int dr \oint \frac{dz}{2ir^2} \left[\frac{\sqrt{BC}}{\sqrt{(z-A)(z-B)(z-C)(z-D)}} + \sqrt{\frac{C^3(z-A)(z-B)}{B(z-C)^3(z-D)^3}} \right]. \quad (\text{A10})$$

Using the same contour without the simple pole at the origin, we obtain the angular part of it as

$$\begin{cases} 4 \left[C_2 E(k) - i C_3 K(k) \right] & \text{for } r > r_0, r'_0 \quad r < r_0, r'_0 \\ -4C_2 \left[E(k) - \frac{(1-k)}{\sqrt{k}} K(1/k) + \sqrt{k} E(1/k) \right] + 4i C_3 \left[K(k) - \frac{K(1/k)}{\sqrt{k}} \right] & \text{for } r_0 < r < r'_0 \end{cases}, \quad (\text{A11})$$

where

$$C_2 = \frac{\sqrt{(r^2 - r_0^2)(r^2 - r'_0^2)}}{(r^2 - r_0 r'_0 e^{i\Delta\theta_0})^2}, \quad (\text{A12})$$

$$C_3 = \frac{r_0 r'_0 \sin \Delta\theta_0}{(r^2 - r_0 r'_0 e^{i\Delta\theta_0}) \sqrt{(r^2 - r_0^2)(r^2 - r'_0^2)}}. \quad (\text{A13})$$

The integral for calculating the density profile in equation (35) is the same as the overlap integral. To calculate the current distribution in equation (36), we have the following integral:

$$-i \int \frac{d\theta}{2r} \left[e^{-i\phi'} \left(\frac{\partial}{\partial\theta} e^{i\phi} \right) - \left(\frac{\partial}{\partial\theta} e^{-i\phi'} \right) e^{i\phi} \right] \quad (\text{A14})$$

$$= \sqrt{\frac{C}{B}} \oint \frac{dz}{4irz} \left(\frac{z}{z-A} + \frac{z}{z-D} - \frac{B}{z-B} - \frac{C}{z-C} \right) \sqrt{\frac{(z-A)(z-B)}{(z-C)(z-D)}}. \quad (\text{A15})$$

The result for $r > r_0, r'_0$ is

$$\frac{\pi}{r} \sqrt{\frac{r_0}{r'_0}} e^{-i\Delta\theta_0/2} + 2C_4 \left[\Pi(n_1, k) - \Pi(n_2, k) \right] + 2C_5 E(k), \quad (\text{A16})$$

where

$$C_4 = \frac{r^2 - r_0 r'_0 e^{-i\Delta\theta_0}}{r \sqrt{(r^2 - r_0^2)(r^2 - r'_0^2)}}, \quad (\text{A17})$$

$$C_5 = \frac{\sqrt{(r^2 - r_0^2)(r^2 - r'_0^2)}}{r(r^2 - r_0 r'_0 e^{i\Delta\theta_0})}. \quad (\text{A18})$$

For $r_0 < r < r'_0$ and $r < r_0, r'_0$, similar substitutions can be performed as in the previous cases.

APPENDIX B: SOME FORMULA WITH ELLIPTIC INTEGRALS

Here is a reminder list of a few definitions of elliptic integrals. $F(\phi, k)$ is the elliptic integral of the first kind,

$$F(\phi, k) = \int_0^\phi \frac{d\theta}{\sqrt{1 - k \sin^2 \theta}}. \quad (\text{B1})$$

$E(\phi, k)$ is the elliptic integral of the second kind,

$$E(\phi, k) = \int_0^\phi d\theta \sqrt{1 - k \sin^2 \theta} . \quad (\text{B2})$$

$\Pi(n, \phi, k)$ is the elliptic integral of the third kind,

$$\Pi(n, \phi, k) = \int_0^\phi \frac{d\theta}{(1 - n \sin^2 \theta) \sqrt{1 - k \sin^2 \theta}} . \quad (\text{B3})$$

The following indefinite integrals are the basic ingredients in the Appendix A. This is the one used for the overlap integral in equation (A2),

$$\int \frac{dz}{z} \sqrt{\frac{(z-a)(z-b)}{(z-c)(z-d)}} = \frac{2(a-b)}{\sqrt{(a-c)(b-d)}} \left[\Pi(n, \phi, k) - \Pi(bn/a, \phi, k) \right] , \quad (\text{B4})$$

where

$$n = \frac{a-d}{b-d} , \quad (\text{B5})$$

$$\phi = \sin^{-1} \sqrt{\frac{(b-d)(z-a)}{(a-d)(z-b)}} , \quad (\text{B6})$$

$$k = \frac{(b-c)(a-d)}{(a-c)(b-d)} . \quad (\text{B7})$$

The next two are used in equation (A10) for the kinetic energy term,

$$\int \frac{dz}{\sqrt{(z-a)(z-b)(z-c)(z-d)}} = \frac{2}{\sqrt{(a-c)(b-d)}} F(\phi, k) , \quad (\text{B8})$$

$$\begin{aligned} \int \frac{dz}{(z-c)(z-d)} \sqrt{\frac{(z-a)(z-b)}{(z-c)(z-d)}} &= \frac{2}{(c-d)^2} \left[\frac{(a-b)(c-d)}{\sqrt{(a-c)(b-d)}} F(\phi, k) \right. \\ &\quad \left. - 2\sqrt{(a-c)(b-d)} E(\phi, k) + (z-a) \frac{(z-c)(b-d) + (z-d)(b-c)}{\sqrt{(z-a)(z-b)(z-c)(z-d)}} \right] . \end{aligned} \quad (\text{B9})$$

The last one is for the current distribution represented by equation (A15),

$$\begin{aligned} \int \frac{dz}{z} \left(\frac{z}{z-a} + \frac{z}{z-d} - \frac{b}{z-b} - \frac{c}{z-c} \right) \sqrt{\frac{(z-a)(z-b)}{(z-c)(z-d)}} &= \frac{4\sqrt{(a-c)(b-d)}}{c-d} E(\phi, k) \\ &\quad + \frac{4(a-b)}{\sqrt{(a-c)(b-d)}} \left[\Pi(n, \phi, k) - \Pi(bn/a, \phi, k) \right] - \frac{2(z-a) \left[(z-c)(b-d) + (z-d)(b-c) \right]}{(c-d)\sqrt{(z-a)(z-b)(z-c)(z-d)}} . \end{aligned} \quad (\text{B10})$$

⁵ H. E. Hall and W. F. Vinen, Proc. Roy. Soc. **A** **238**, 204 (1956).

⁶ H. E. Hall and W. F. Vinen, Proc. Roy. Soc. **A** **238**, 214 (1956).

⁷ V. L. Berezinskii, Zh. Eksp. Teor. Fiz. **59**, 907 (1970), [Sov. Phys. JETP **32**, 493 (1971)].

⁸ J. M. Kosterlitz and D. J. Thouless, J. Phys. C **6**, 1181 (1973).

⁹ S. H. Lamb, *Hydrodynamics* (The University Press, Cambridge, 1932).

¹⁰ R. J. Donnelly, *Quantized Vortices in Helium II* (Cambridge University Press, New York, 1991).

¹¹ G. W. Rayfield and F. Reif, Phys. Rev. **136**, A1194 (1964).

¹² P. Nozières and D. Pines, *The Theory of Quantum Liquids II* (Addison-Wesley, Reading, 1990), pp. 88-95.

¹³ D. J. Thouless, P. Ao, and Q. Niu, Phys. Rev. Lett. **76**, 3758 (1996).

¹⁴ J. M. Duan, Phys. Rev. B **48**, 333 (1993).

¹⁵ Q. Niu, P. Ao, and D. J. Thouless, Phys. Rev. Lett. **72**, 1706 (1994).

¹⁶ J. M. Duan, Phys. Rev. B **49**, 12381 (1994).

¹⁷ J. M. Duan, Phys. Rev. Lett. **75**, 974 (1995).

¹⁸ Q. Niu, P. Ao, and D. J. Thouless, Phys. Rev. Lett. **75**, 975 (1995).

¹⁹ G. V. Chester, R. Metz, and L. Reatto, Phys. Rev. **175**, 275 (1968).

²⁰ E. P. Gross, Nuovo Cimento **20**, 454 (1961).

²¹ L. P. Pitaevskii, Zh. Eksp. Teor. Fiz. **40**, 646 (1961), [Sov. Phys. JETP **13**, 451 (1961)].

²² A. L. Fetter, Phys. Rev. Lett. **27**, 986 (1971).

²³ M. Saarela and F. V. Kusmartsev, Phys. Lett. A **202**, 317 (1995).

²⁴ G. Ortiz and D. M. Ceperley, Phys. Rev. Lett. **75**, 4642 (1995).

²⁵ S. A. Vitiello, L. Reatto, G. V. Chester, and M. H. Kalos, Phys. Rev. B **54**, 1205 (1996).

²⁶ S. Giorgini, J. Boronat, and J. Casulleras, Phys. Rev. Lett. **77**, 2754 (1996).

²⁷ M. Sadd, G. V. Chester, and L. Reatto, Phys. Rev. Lett. **79**, 2490 (1997).

²⁸ D. L. Hill and J. A. Wheeler, Phys. Rev. **89**, 1102 (1953).

²⁹ M. G. Redlich and E. P. Wigner, Phys. Rev. **95**, 122 (1954).

³⁰ R. E. Peierls and J. Yoccoz, Proc. Roy. Soc. A **70**, 381 (1957).

³¹ R. E. Peierls and D. J. Thouless, Nucl. Phys. **38**, 154 (1962).

³² R. A. Ashton and W. L. Glaberson, Phys. Rev. Lett. **42**, 1062 (1979).

³³ R. P. Feynman, Phys. Rev. **94**, 262 (1954).

³⁴ B. E. Clements, J. L. Epstein, E. Krotscheck, and M. Saarela, Phys. Rev. B **48**, 7450 (1993).

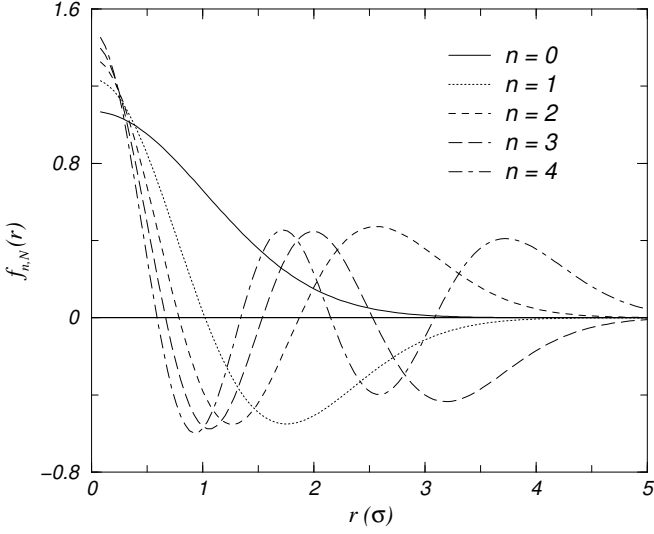


FIG. 1. The weighting functions for the angular momentum $l = N$, where the normalization is chosen such that $\int dr f(r)^2 = 1$. The state of the first Landau level ($n = 0$) can be fitted by $e^{-r^2/2}$.

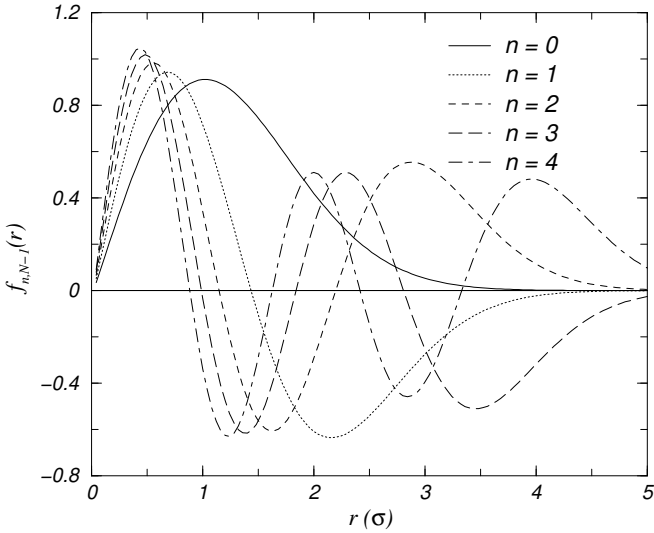


FIG. 2. The weighting functions for the angular momentum $l = N - 1$. The state of the first Landau level ($n = 0$) can be fitted by $re^{-(r-1)^2}$.

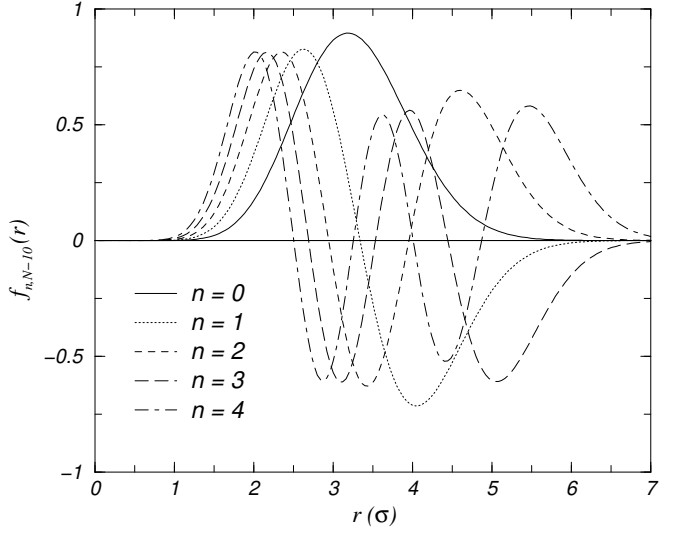


FIG. 3. The weighting functions for angular momentum $l = N - 10$. The state of the first Landau level ($n = 0$) can be fitted by a Gaussian $e^{-(r-r_v)^2}$, where r_v is very close to $\sqrt{10}$ as expected.

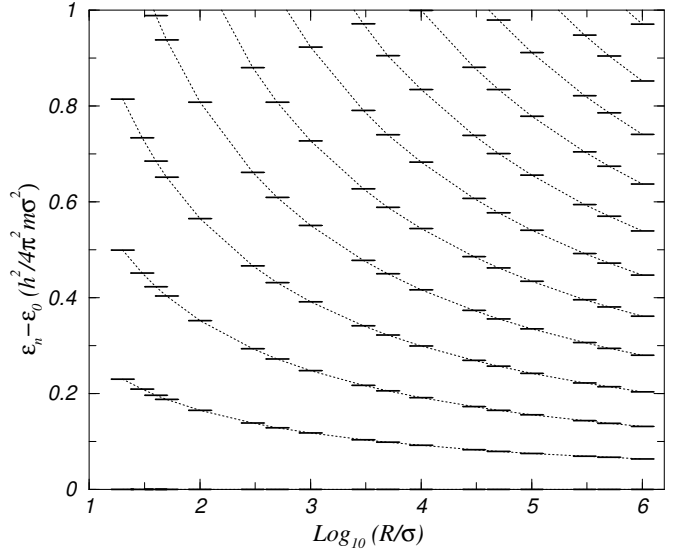


FIG. 4. The energy spectrum corresponding to the cyclotron motion relative to the first Landau level. The dotted lines show the scaling of the Landau levels with the system radius ranged from $R = 20$ to $R = 10^6$. The same spectrum is obtained for any given angular momentum.

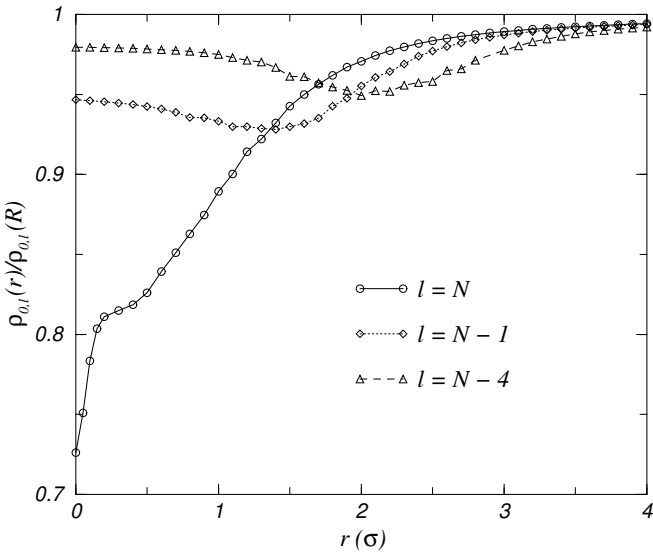


FIG. 5. The radial density profiles for three states with different angular momenta in the first Landau level at system radius $R = 10$. The normalization scheme is choosing the asymptotic density to be unity rather than keeping the total number of particles fixed.

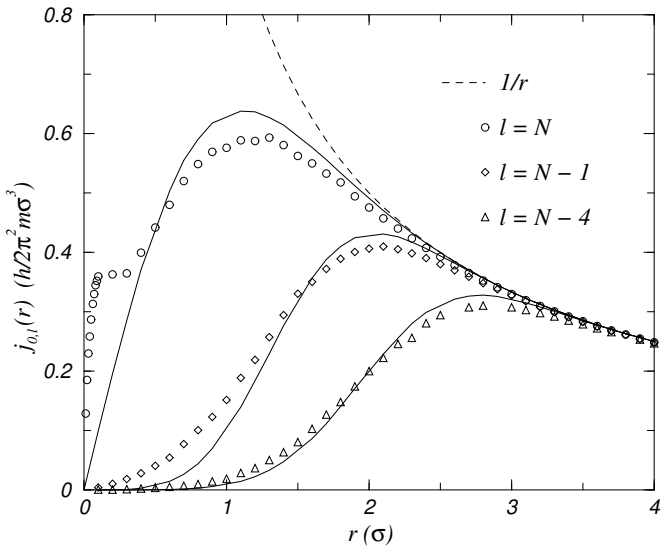


FIG. 6. The radial current distributions for three states with different angular momenta in the first Landau level. The symbols represent the numerical results at system radius $R = 10$ and the solid lines are the analytic approximation for the infinite system.

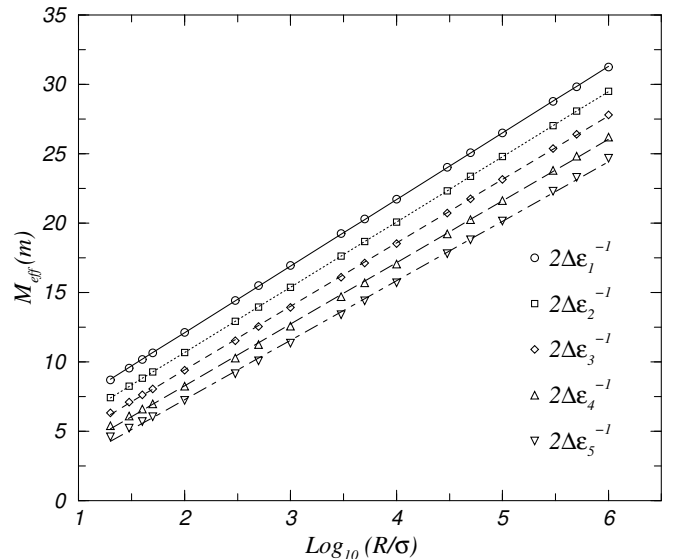


FIG. 7. The scalings of the inverse Landau-level spacings labeled as $\Delta E_n = E_{n+1} - E_n$. They are related to the effective mass in the point-particle picture of a vortex. The symbols show the first five of them from top to bottom. The lines are the least-square fittings and clearly show that the effective mass scales logarithmically with the system size.

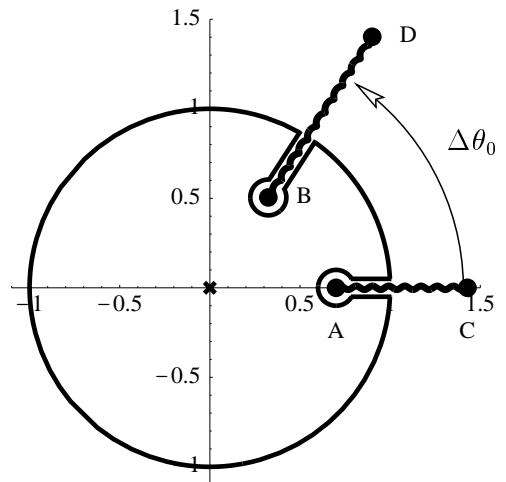


FIG. 8. The integration contour deformed from the unit circle. There are always two branch points inside the unit circle, and two outside. The labelling from A to D shows a particular choice of $r > r_0, r'_0$. There may be a simple pole located at the origin depending on which integrand is discussed.